J. Basic. Appl. Sci. Res., 2(5)4529-4541, 2012

ISSN 2090-4304
Journal of Basic and Applied Scientific Research
www.textroad.com

A Simple Position Sensorless Control Strategy for Radial-Flux Brushless DC Motor Drives Using Single Current Sensor

Mohsen Ebadpour[1], Mohammad Reza Feyzi[2], Mohammad Bagher Bannae Sharifian[2], Mohammad Reza Alizadeh Pahlavani[3]

[1] Ilkhchi Branch, Islamic Azad University, Ilkhchi, Iran
[2] Faculty of Electrical and Computer Engineering, University of Tabriz, Tabriz, Iran
[3] Malek-Ashtar University of Technology (MUT), Shabanlo St., Lavizan, Tehran, Iran

ABSTRACT

Reducing the cost of the motor drive is desirable for low cost applications. A simple and cost-effective position sensorless control for radial-flux permanent magnet brushless DC (BLDC) motor drives using single current sensor is proposed in this paper. It is based on the generation of quasi-square current waveforms, using only one current controller for the three phases. Unlike the conventional methods, the proposed method presents advantages such as very simple control scheme, without needing to triangular carrier modulation, and balanced phase currents. The proposed position sensorless technique is based on the detection of zero crossing points of three voltage functions that are derived from the difference between the lines' voltage measured at the terminals of the motor. In order to improve the speed transient response of the BLDC motor and enhance the energy saving aspect of the system, it should enjoy a high quality dynamic response characteristic. Therefore, to realize these purposes, particle swarm optimization (PSO) has been proposed to regulate the proportional-integral-derivative (PID) parameters of the motor speed controller. The proposed control algorithm is particularly suitable for cost sensitive product such as air purifiers, air blowers, cooling fan, and related home applications. The effectiveness of the proposed system has been validated by comparative studies and simulation results.
KEY WORDS: Cost-effective drive, radial-flux brushless DC (BLDC) motor- position sensorless control- single current sensor- particle swarm optimization (PSO).

1. INTRODUCTION

Radial-flux permanent magnet brushless DC (BLDC) motors are being used increasingly in computers, automotive, industrial and household products because of their high power density, compactness, high efficiency, low maintenance, and ease of control. Minimizing the cost of the motor drives is the key factor of low cost applications. Nowadays, most commercial PM drives are based on current control strategies. However, sensors and their associated accessories increase complexity, cost, and size of the motor drives and reduce the reliability of the system. Therefore, reduction of the number of sensors is desirable in motor drives. The most appealing current sampling method for BLDC motor is using only one current sensor. The easiest method is using a DC-link current sensor.

Some single current control strategies have been studied on BLDC motor drives [1-8]. The single-current-sensor sliding mode driving strategy for four-switch three-phase brushless DC motor was proposed in [4]. It introduced two kinds of methods based on phase plane portrait and Taylor-series expansion to determine the sliding mode plane convergence domain. In [5], a simple novel digital pulse width modulation control to develop a low cost controller for domestic applications has been implemented for a trapezoidal BLDC motor drive system with a single current sensor. A modified DC link current sensor was proposed in [6]. It adds an inductance in the upper DC bus to stabilize the current flowing through the current sensor during a Pulse Width Modulation (PWM) period. Although it is helpful to evaluate the phase current without needing to any PWM strategy information, the existence of inductance tends to prevent the desired current regulation in phases. So this method is not suitable for current loops. Another current sensor was proposed in [7]; it works well at any instant despite the PWM strategy used. The key theory of this method is collecting both the freewheeling current through the antiparallel freewheeling diode and the DC link current. Therefore, it will not lose any current

***Corresponding Author:** Mohsen Ebadpour, Ilkhchi Branch, Islamic Azad University, Ilkhchi, Iran
Email: m.ebadpour@yahoo.com, m.ebadpour@ieee.org

information during a PWM period. But in this case, the freewheeling current in the closing phase is still a torque source and produces torque ripple in the commutation region.

Another method proposed in [8], is suitable for PWM strategies. However, this improved method still has some disadvantages, since discrete freewheeling diodes have to be used to circulate motor reactive currents following the openings of the inverter switches, and the effect of the antiparallel freewheeling diode integrated into a power switch must be eliminated by another discrete diode connected in series with the switches. Therefore, this method increases the size of inverter.

Conventional BLDC motor drives are generally implemented via a six-switch three-phase inverter, three Hall Effect position sensors and two current sensors that generate proper signals for current commutation [9]. However, it is a well known fact that these sensors have a great number of drawbacks; they increase the cost of the motor and require special mechanical arrangements to be mounted. In addition, Hall sensors are temperature-sensitive and hence limit the operation of the motor. They can reduce system reliability because of their extra components and wiring. Furthermore, sensorless control is the reliable way to operate the motor for applications in harsh environments. During the last two decades, a lot of researches on sensorless control techniques of BLDC motors have been conducted. This research can be divided into four categories [10]. 1) Detecting the zero crossing points of the motor terminal to neutral voltage with or without precise phase shift circuit [11, 12]. 2) Back electromagnetic force (EMF) integration method [13]. 3) Sensing the third harmonic of the back EMF [14]. 4) Detecting the freewheeling diode conduction and related extensive strategies [15]. Among the various techniques, the back EMF zero crossing detection method is most popular due to its simplicity, ease of implementation, and lower cost [16, 17].

In this paper, a cost-effective position sensorless control for BLDC motor drives using a single current sensor is proposed. The proposed control strategy is based on just one hysteresis current controller and a PSO tuned PID controller for speed regulation. The position sensorless method relies on a difference between the lines' voltage measured at the terminals of the motor. The main motivation of this paper is to show that replacing conventional current control methods with a simple single current control strategy without using position sensors, and reducing the cost and size of the motor drives. Furthermore, optimization of the BLDC motor drives has been proposed by the PSO optimized PID speed controller.

2. ANALYSIS OF THE THREE-PHASE RADIAL-FLUX BLDC MOTOR

Permanent magnet DC motors use mechanical commutator and brushes to achieve the commutation. However, BLDC motors adopt Hall-Effect sensors in place of mechanical commutator and brushes. The stators of BLDC motors are the coils, and the rotors are the permanent magnets. The stators develop the magnetic fields to make the rotor rotating. Hall-Effect sensors detect the rotor position as the commutating signals. Therefore, the BLDC motors use permanent magnets instead of coils in the armature and so do not need brushes. In this paper, a three-phase, two-pole BLDC motor is used. Configuration of BLDC motor drive system is shown in Fig. 1.

BLDC motor is driven by a three-phase inverter with so called ''six-step commutation''. The conducting interval for each phase is 120 electrical degrees. The commutation phase conducting sequence appears as S_5–S_6, S_1–S_6, S_1–S_2, S_3–S_2, S_3–S_4, and S_5–S_4 where, each conducting stage is called one step. Therefore, only two phases are energized in each step, leaving the third phase floating. In order to produce maximum torque, the inverter should be commutated every 60° so that current remains in phase with the back-EMF. The commutation times are governed by the rotor position that can be either detected by appropriate sensors, or estimated from motor parameters in a sensorless system [18]. For a three phases BLDC motor the back-EMF and phase current waveforms with 120° conduction mode are shown in Fig. 2. In the work presented here, the analysis is based on the following assumption for simplification:

(1) Concentrated stator windings are placed with a 120° positional difference to each other, and they are connected in wye.
(2) Stator windings are symmetric and the windings resistance and inductance are assumed to be constant.
(3) Magnetic saturation, hysteresis and eddy current losses are ignored.
(4) Armature reaction is ignored and air gap distribution is assumed to be uniform.

Under the above assumption, the analysis of a BLDC motor is described as following equations:

$$\begin{bmatrix} v_a \\ v_b \\ v_c \end{bmatrix} = \begin{bmatrix} R & 0 & 0 \\ 0 & R & 0 \\ 0 & 0 & R \end{bmatrix} \begin{bmatrix} i_a \\ i_b \\ i_c \end{bmatrix} + \begin{bmatrix} L & 0 & 0 \\ 0 & L & 0 \\ 0 & 0 & L \end{bmatrix} \frac{d}{dt} \begin{bmatrix} i_a \\ i_b \\ i_c \end{bmatrix} + \begin{bmatrix} e_a \\ e_b \\ e_c \end{bmatrix} + \begin{bmatrix} v_N \\ v_N \\ v_N \end{bmatrix} \tag{1}$$

$$v_{aN} = v_a - v_N,\ v_{bN} = v_b - v_N,\ v_{cN} = v_c - v_N \tag{2}$$

$$L = (L_S - L_M) \tag{3}$$

where v_a represents terminal phase a voltage with respect to the power ground, i_a is the rectangular-shaped phase a current, e_a is the trapezoidal-shaped back EMF, v_N is the neutral-point voltage with respect to the power ground, and R, L_S and L_M are resistance, self-inductance and mutual-inductance, respectively.

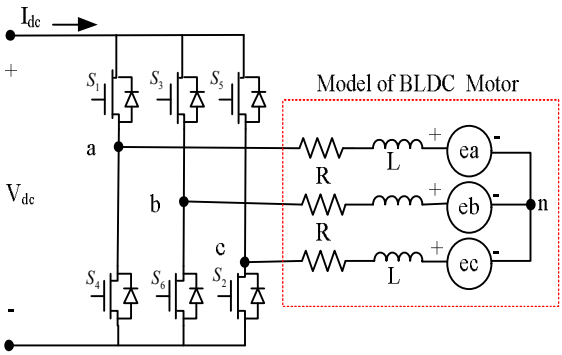

Fig. 1. The structure of BLDC motor

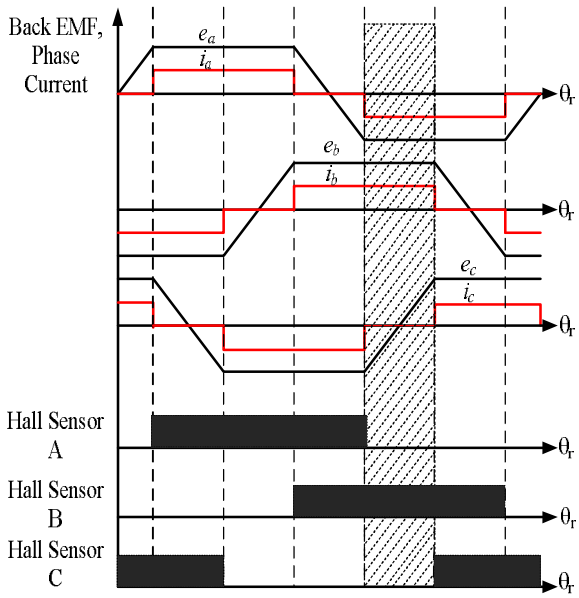

Fig. 2. Signal waveforms in the BLDC motor

The electromagnetic torque is expressed as:

$$T_e = \frac{1}{\omega_r}(e_a i_a + e_b i_b + e_c i_c) \tag{4}$$

where ω_r is the mechanical speed of the rotor. Fig. 2 shows trapezoidal back EMF, current profiles, and Hall sensor signals of the three-phase BLDC motor drive. The current phase generation is a "120° ON and 60° OFF" type.

3. PSO ALGORITHM AND PID CONTROLLER DESIGN

3.1. PSO Algorithm

Particle Swarm Optimization first proposed by Kennedy and Eberhart [19]. PSO is a form of evolutionary computation technique based on natural systems. Each particle in the population is a feasible solution. Optimal regions of complex search spaces are found through the interaction of individuals in the population. The key advantages of PSO over other optimization techniques are as follows: lower sensitivity to the nature of the objective function, derivative free property unlike many conventional techniques, easy implementation.

The algorithm starts with *N* particles. Each particle represents a candidate solution to the problem. Each particle in the search space has a current position X_i and a current velocity V_i. The value of each particle is determined by the fitness function $F(X_i)$. Each particle moves about the cost surface with a velocity. The personal best position in search space $localbest_i$ corresponds to the position where particle *i*, represents the best fitness function. The global best position in search space *globalbest* represents the position yielding the best fitness function amongst all $localbest_i s$.

The steps of the algorithm are as follows:

a) Formatting of the initial population and initial velocities randomly.
b) Calculating the value of each particle by the fitness function.
c) Finding local best of each particle.
d) Finding global best of all populations.
e) The PSO algorithm updates the velocity for each particle then adds that velocity to the particle position or value.

Velocities updates are influenced by the both best global solution associated with the lowest cost ever found by a particle and the best local solution associated with the lowest cost in the present population according to (5) and (6) as follows:

$$X_i^{n+1} = X_i^n + V_i^{n+1} \tag{5}$$

$$V_i^{n+1} = V_i^n + \rho_1 . r_1 . (X_i^{localbest} - X_i^n) + \rho_2 . r_2 . (X_i^{globalbest} - X_i^n) \tag{6}$$

In these equations, super script *n+1* denotes *n+1*th iteration and super script *n* denotes nth iteration. Where X_i denotes the *i*th particle and V_i is the velocity correspond to this particle. Also, ρ_1, ρ_2 are learning factors and r_1, r_2 are independent uniform random numbers. $X_i^{localbest}$ is the best local solution for the *i*th particle and $X_i^{globalbest}$ is the Best global solution. Steps *b* to *e* are repeated until termination criteria satisfies [20].

3.1. PID Controller Design and Problem Formulation

The PID controller is used to improve the dynamic response and reduce the steady-state error. The transfer function of a PID controller is described as:

$$G_c(s) = k_p + \frac{k_i}{s} + k_d s \tag{7}$$

where k_p, k_i and k_d are proportional, integral and derivative gains, respectively. System response can be evaluated by overshoot (M_p), rise time (t_r), settling times (t_s), and steady-state error (E_{ss}). To improve the system performance by considering these parameters, an objective function is defined. The objective function will be minimized by an appropriate regulation of PID parameters (k_p, k_i, k_d). By minimizing the objective function, desired transient response to load disturbance is achieved [21]. The objective function can be defined as:

$$f(K) = (1 - e^{-\beta})(M_p + E_{ss}) + e^{-\beta}(t_s - t_r) \tag{8}$$

where *K* is [k_p, k_i, k_d] and β is the weight factor. Decreasing rise time and settling time can be achieved by using a weight factor smaller than 0.7 and increasing this parameter higher than 0.7, will lead to reduction in overshoot and steady state error.

Because of the system's nonlinear behavior, the objective function should be minimized by intelligent algorithms. Nowadays, the PSO algorithm is one of the fastest and most accurate methods in

comparison with other intelligent algorithms. So in this paper, it is utilized to achieve optimal PID controller parameters using MATLAB software. PSO results for iteration= 20 and weight factor= 0.5 are shown in the table 1.

TABLE 1. Best PID Controller with β=0.5 Value Gained by PSO Algorithm

BLDCM				
B	***Iteration***	k_p	k_i	k_d
0.5	20	10	25	0.9
M_p	E_{ss} *(%)*	t_r*(sec)*	t_s*(sec)*	***Min Cost***
0	0.22	0.007	0.021	0.0084

4. POSITION SENSORLESS SCHEME

4.1 Back EMF Zero Crossing Estimation Method

The proposed position sensorless BLDC motor drive, is based on the detection of back EMF zero crossing from the terminal voltages, similar to the sensorless technique used in [22]. Considering a BLDC motor with three stator phase windings connected in star. The BLDC motor is driven by a six-switch three-phase inverter in which the switches are triggered with respect to the rotor position as shown in Fig. 2. Phase *a* terminal voltage with respect to the star point of the stator and according to (1) is given in as:

$$v_{aN} = Ri_a + L\frac{di_a}{dt} + e_a \tag{9}$$

Similar equations can be written for the other two phases, as in (10) and (11)

$$v_{bN} = Ri_b + L\frac{di_b}{dt} + e_b \tag{10}$$

$$v_{cN} = Ri_c + L\frac{di_c}{dt} + e_c \tag{11}$$

From these equations, line voltage v_{ab} may be determined as:

$$v_{ab} = v_{aN} - v_{bN} = R(i_a - i_b) + L\frac{d(i_a - i_b)}{dt} + e_a - e_b \tag{12}$$

Similarly:

$$v_{bc} = R(i_b - i_c) + L\frac{d(i_b - i_c)}{dt} + e_b - e_c \tag{13}$$

$$v_{ca} = R(i_c - i_a) + L\frac{d(i_c - i_a)}{dt} + e_c - e_a \tag{14}$$

These line voltages can, however, be estimated without the need for star point by taking the difference of terminal voltages measured with respect to the negative DC bus. Subtracting (14) from (13) gives:

$$v_{bcca} = R(i_b - 2i_c + i_a) + L\frac{d(i_b - 2i_c + i_a)}{dt} + e_b - 2e_c + e_a \tag{15}$$

Consider the interval when phases *a* and *b* are conducting and phase *c* is open as indicated by the shaded region in Fig. 2. In this interval, phase *b* winding is connected to the positive polarity of the DC supply, phase *a* to the negative polarity of the DC supply and phase *c* is open. Therefore $i_b = -i_a$ and $i_c = 0$. It can be seen from Fig. 2 (shaded region) that the back EMF in phases *a* and *b* are equal and opposite. Therefore, in that interval, (15) may be simplified as:

$$v_{bcca} = e_b - 2e_c + e_a = -2e_c \tag{16}$$

Thus, the back EMF of phase *c* may be estimated. It is again evident from Fig. 2 that during this interval (shaded region) the back EMF e_c transients from one polarity to another zero crossing. Therefore, operation v_{bcca} enables the detection of zero crossing of phase *c* back EMF. Similarly, the difference of line-to-line voltage v_{abbc} enables the detection of zero crossing of phase *b* back EMF when phases *a* and *c* back EMFs are equal and opposite. The difference of line-to-line voltage v_{caab} waveform gives the zero crossing of phase *a* back EMF, where phases *c* and *b* have equal and opposite back EMFs.

Therefore, the zero crossing instants of the back EMF waveforms may be estimated indirectly from measuring only the three terminal voltages of the motor. By means of the estimated back EMFs, virtual Hall sensor signals are made as shown in Fig. 3.

Fig. 4 shows the simulated back EMF waveform of phase *c*, the line voltage difference v_{bcca} and virtual Hall sensor signal of phase *c*. As shown in Fig. 4(a), the v_{bcca} waveform contains voltage spikes appearing at the commutation instants. These voltage spikes are the result of conduction of the free-wheeling diode at the phase commutation instants and are to be filtered out. Otherwise they cause unwanted zero crossing points. To eliminate this, three low pass filters typed Butterworth order 2 with a cut off frequency of about 500 rad/sec are chosen.

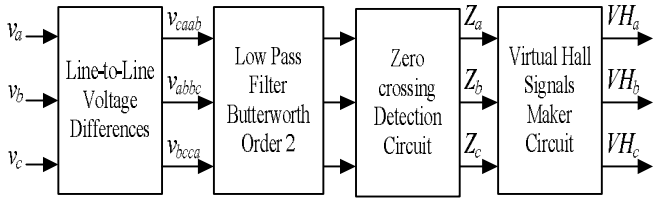

Fig. 3: Functional sequence of the operations in the proposed back EMF Zero Crossing Estimation Method

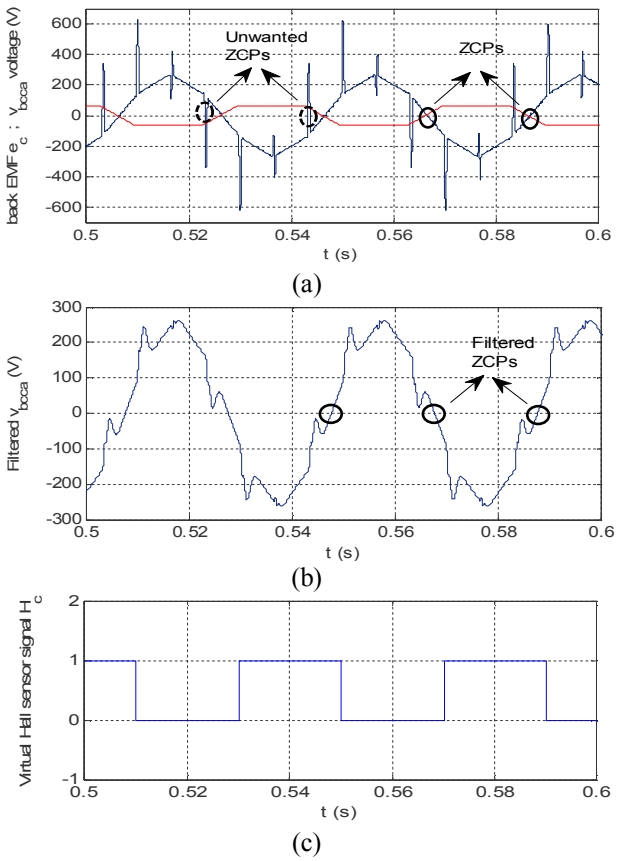

Fig. 4: Detection of back EMF zero crossing, (a) Unfiltered v_{bcca} voltage waveform and back EMF of phase *c*, (b) Filtered v_{bcca} voltage waveform, (c) Virtual Hall sensor signal H_c

4.1. Starting Technique

The sensorless schemes are not self-starting. In order to sense the back EMF, the motor must be first started and brought up to a certain speed where the back EMF voltage can be detected. In practice, open-loop starting the motor is accomplished by providing a rotating stator field with a certain increasing frequency profile [23]. Once the stator field begins to attract the rotor field enough to overcome friction and inertia, the rotor will turn. After the speed reaches a threshold voltage value, the back EMF can be

detected providing position information, the system switches to synchronous commutation mode and the motor acts as a permanent magnet synchronous machine.

When the motor stops, the rotor initial position is undefined for the controller. The first step is to align the motor to a known position by exciting the two phases of the motor. For instance, we can choose phases A and B to be excited to set the initial position. After the rotor located in the initial position, a preset exciting pattern is sent out. If the three phases are alternately excited, the motor will start to accelerate. Table 2 show the exciting pattern for forward rotation. The motor is driven with 6-step mode, and the exciting phase just repeats the same pattern after one cycle (6 steps).

TABLE 2. Phase Exciting Pattern for Forward Rotation

	Alignment (Step 0)	Step 1	Step 2	Step 3	Step 4	Step 5
Exciting phases	AB	AC	BC	BA	CA	CB

5. PROPOSED CONTROL SYSTEM DESCRIPTION

The common control algorithm for a BLDC motor is PWM current control. It is based on the measurement of phase current, which is compared and forced to follow a quasi-square template. This method requires an appropriate current reference, which can be relatively complex and difficult to implement. Fig. 5 shows a schematic of the proposed control strategy. The operation of the system is as follows:

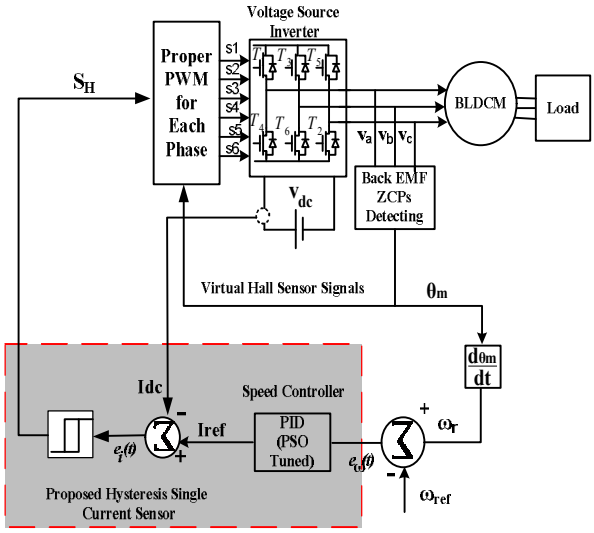

Fig. 5: Overall block diagram of proposed strategies

As the motor is a brushless DC type, the waveforms of armature currents are quasi-square. For control of speed and armature currents of motor, first, the speed of the motor is compared with its reference value. The speed error can be represented as:

$$e_{\omega}(t) = \omega_{ref} - \omega_r(t) \tag{17}$$

where ω_{ref} is the reference speed value and $\omega_r(t)$ is the measured speed value at time t. The speed error is processed in the PID speed controller, tuned by PSO algorithm. The output of the speed PID controller is the reference torque value, but, According to this relation:

$$I_{ref} = T_{ref} / K_t \tag{18}$$

where T_{ref} and K_t are the reference torque and torque constant respectively, the output of speed controller is considered as the reference current (I_{ref}). Then, the measured DC-link current is compared with the reference current. The input of the current controller is:

$$e_i(t) = I_{ref}(t) - I_{dc}(t) \tag{19}$$

From this comparison, current error signal $e_i(t)$ is obtained. This error passing through a simple hysteresis current controller directly generates chopping for all six power switches of the inverter, which are sequentially active by the hall-effect sensor. Ultimately the hysteresis current controller regulates the

winding currents within the small band around the DC reference current. The electromagnetic torque is directly commanded by current reference. The larger the current reference, the higher torque produced. Also restriction is expelled on the PID speed controller output depending on the permissible maximum winding currents. This expelled restriction causes a good compatibility with practical control systems.

6. REVIEW OF TWO CONVENTIONAL SINGLE CURRENT CONTROL METHODS

In general, current control strategies for BLDC motor drives can be divided into three topologies: hysteresis band control, PWM control, and variable DC-link voltage control. In this section, two conventional methods i.e. the PWM control and the variable DC-link voltage control are explained.

6.1 PWM Control

In PWM control the motor is turned on and off at a high rate. The chopping frequency is fixed but the length of the duty cycle depends on the control error. The fact that the frequency is fixed, makes filtering of acoustic and electromagnetic noise easier. The switching frequency is commonly 20-50 kHz. The three PWM strategies generally used in BLDC motor drives are double-sided basic PWM, single-sided PWM and double-sided complementary PWM [6]. It should be noted that some PWM techniques cause circulating current in the floating phase. This results in torque error with higher torque ripple and thus, reduction of efficiency. It also makes a DC-link current sensor unfavorable [24]. Although a bipolar PWM modulation technique such as H_PWM_L_PWM does not generate circulating current in the floating phase, but it increases switching loss in the power circuit and winding loss due to high ripple current in the motor windings [25]. On the other hand, although unipolar PWM modulation techniques such as PWM_ON, ON_PWM, and PWM_ON_PWM give low switching loss, ripple current still exists and this produces a torque ripple [26].

In addition, in this scheme, the duty cycles of the switches are interdependent. Therefore, it may cause commutation delay or an irregular switching frequency of the power devices in a high speed sensorless control.

6.2 Variable DC-Link Voltage Control

Using a variable DC voltage source to control the applied voltage, can have some advantages over the PWM control scheme. A linear power stage is cheaper than a pulsed power stage (PWM) but the losses can be high at a low voltage and high current. However, at a high speed, a linear power stage can be the best alternative when switching losses and commutation delay of a pulsed power stage are significant [27].

The variable DC-link voltage technique is the only technique that does not cause high frequency disturbances; at least if it is assumed that the variable voltage sources are ideal. Its performance is similar to the PWM method but it produces much smoother torque due to the absence of high frequency switching. In the frequency domain, the variable DC-link voltage technique contains only harmonics caused by current commutation.

7. SIMULATION RESULTS AND COMPARATIVE STUDIES

To evaluate the performance of the proposed system it is compared with the two conventional current control strategies for the same condition, and simulation models have been established using MATLAB/SIMULINK. The sampling interval is 5μsec, the magnitude of the current hysteresis band and the switching frequency in the conventional PWM control scheme are 0.2A and 20 kHz, respectively. The simulation parameters of a surface mounted magnet BLDC motor are given in Table 3.

TABLE 3. Simulation Parameters of the BLDC Motor

Parameters	Value
Phase resistance	0.4Ω
Phase inductance	13mH
Rated speed	1500 rpm
dc-link voltage	300V
Pole pairs	1
Rated torque	3 N.m
Inertia	0.004 (kg.m^2)
Friction factor	0.002 (N.m.s)
Torque constant	0.4V/(rad/sec)

7.1 Comparative Studies in the Single Current Control Strategy

In this section, the BLDC motor phase currents for each mentioned strategies are depicted in Fig. 6. The square waveforms of phase currents using the proposed method (Fig. 6(c)) verify the well control capability of the BLDC motor compared to the two other conventional methods. As shown in Fig. 6(c), current spikes in the commutation region and current ripple in the conduction region are eliminated effectively.

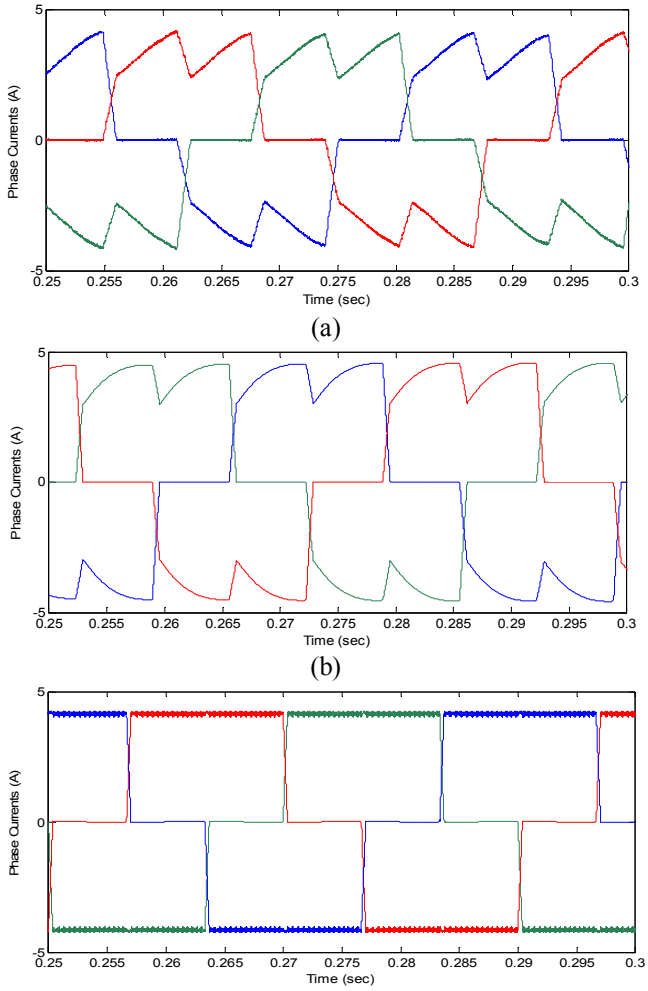

Fig. 6: Motor phase currents a) PWM control b) Variable DC link voltage control scheme c) proposed method.

The BLDC motor electromagnetic torques is shown in Fig. 7. Since there is a linear relationship between the phase current and electromagnetic torque in BLDC motors, current ripple in the proposed strategy is reduced. Therefore, torque ripple has been reduced. As shown in Fig. 7(c), the percentage of torque ripple in the proposed strategy is about 2.7 while, in PWM control and the variable DC link voltage control scheme are 24 and 20, respectively.

PSO has been used to regulate the PID parameters of speed controller. As shown in Fig. 8(c), the speed response characteristic has been completely satisfied to have no overshoot, and has small rise and settling times with respect to the conventional control strategies. The obtained high performance speed response for the BLDC motor is differentiated by circle region in Fig. 8(c).

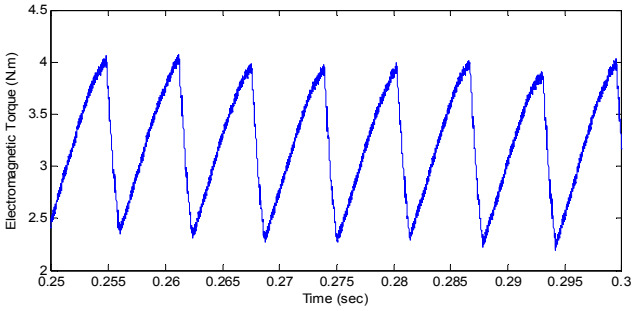

(a)

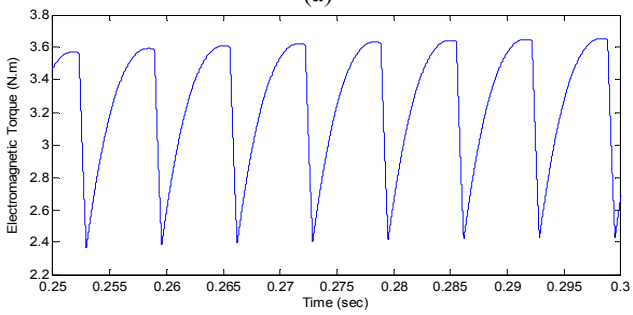

(b)

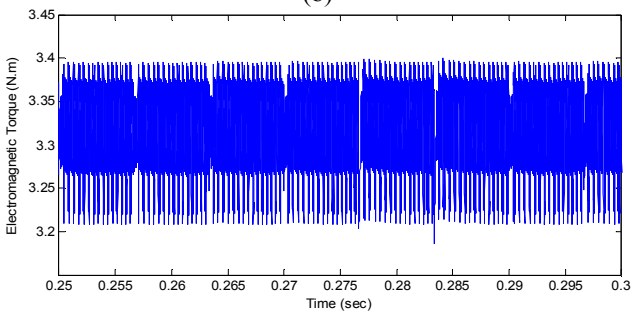

(c)

Fig. 7: The electromagnetic torques a) PWM control b) Variable DC link voltage control scheme c) proposed method.

7.2 Position Sensorless Control of BLDC Motor Drives Using Single Current Sensor

Fig. 9 shows the position sensorless operation of the BLDC motor in its rated speed (1500 rpm) and full load condition (3 N.m). Fig. 9(a,b) shows the speed and developed electromagnetic torque. It is clear that speed tracking is well and the developed torque has very low ripple. Moreover, the currents are quasi-square waveforms with some low ripples as shown in Fig. 9(c).

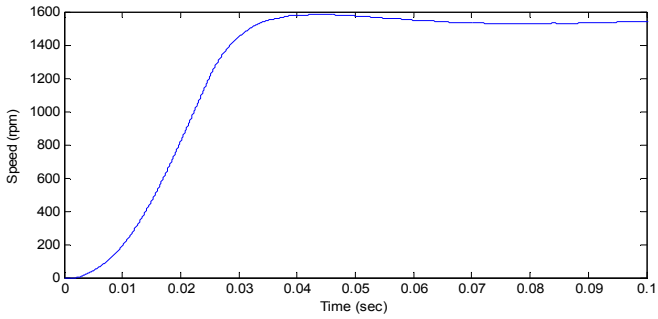

(a)

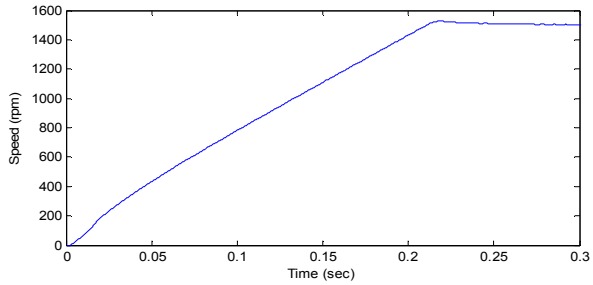

(b)

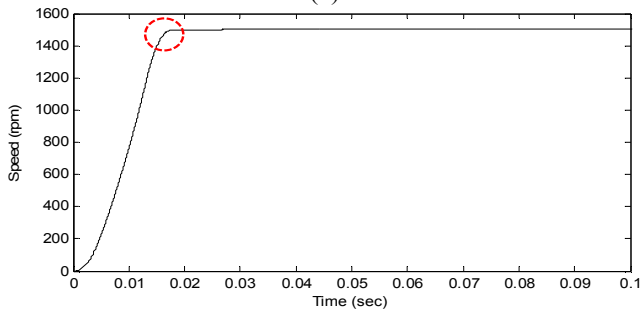

(c)

Fig. 8: The speeds of rotor a) PWM control b) Variable DC link voltage control scheme c) proposed method.

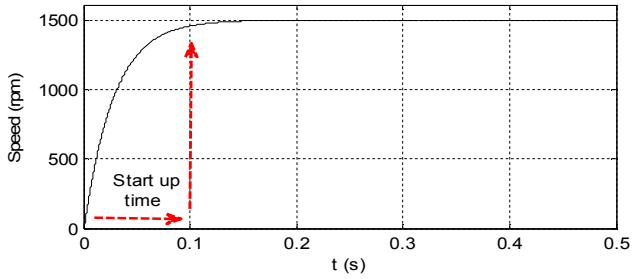

(a)

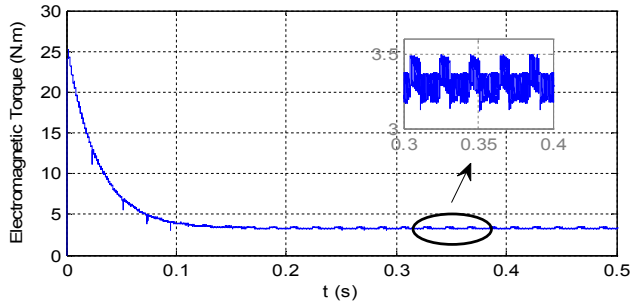

(b)

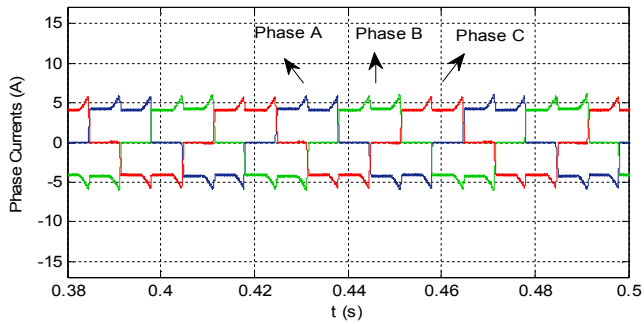

(c)

Fig. 9: Position sensorless control at speed 1500 rpm and full load condition. (a) speed, (b) developed electromagnetic torque, (c) phase current waveforms

8. CONCLOSION

A cost effective, higher performance radial-flux permanent magnet BLDC motor drive system has been proposed. To sample the phase current at any instant, an effective single current sensor technique without the need for information of freewheeling current or current sign has been adopted. Therefore, the size of the motor drive is reduced. Virtual Hall sensor signals are made by detection of zero crossing points of the difference of line voltage measured at the terminals of the motor. In the proposed sensorless scheme, no phase shift is required, which is prevalent in most of sensorless algorithms. Compared to the conventional BLDC motor drive scheme, it is not complicated and eliminates the use of complex hardware. This simple drive system can improve torque performance in BLDC motor drives. A PSO tuned PID controller is also used to improve the dynamic response and reduce the steady-state speed error. Finally, the proposed strategy has been successfully verified by simulation results. The simulation results include two parts; comparative studies in the single current control strategy and position sensorless control of BLDC motor drives using single current sensor.

9. REFERENCES

[1] M. Ebadpour, M. B. B. Sharifian, M. R. Feyzi, 2011. A cost-effective position sensorless control for four-switch three-phase brushless DC motor drives using single current sensor. International Review of Automatic Control (I.RE.A.CO.), 4 (3): 386-393.

[2] M. R. Feyzi, M. Ebadpour, S. A. KH. Mozaffari Niapour, A. Feizi, R. Mousavi Aghdam, 2011. A new single current strategy for high-performance brushless DC motor drives. in Proc. IEEE 24th Canadian Conference on Electrical and Computer Engineering (CCECE 2011), 000419-000424.

[3] C. Xia, Z. Li, T. Shi, 2009. A control strategy for four-switch three-phase brushless DC motor using single current sensor. IEEE Trans. Industrial Electronics, 56 (6): 2058-2066.

[4] F. Qiang, L. Hui, Z. Hai-tao, 2007. Single-current-sensor sliding mode driving strategy for four-switch three-phase brushless DC motor. in Proc. ICTT 2006, 2396-2401.

[5] A. Sathyan, M. Krishnamurthy, N. Milivojevic, A. Emadi, 2099. A low-cost digital control scheme for brushless DC motor drives in domestic applications. in Proc. IEMDC'09, 76-82.

[6] H. Tan and S. L. Ho, 1999. A novel single current sensor technique suitable for BLDCM drives. in Proc. Power Electronics and Drive Systems, PEDS '99, 133-138.

[7] P. P. Acarnley, 1993. Current measurement in three-phase brushless DC drives. Electronic Power Applications, IEE Proceedings-B 140 (1): 71-79.

[8] F. Blaabjerg, J. K. Petersen, U. Jaeger, and P. Thoegersen, 1992. Single current sensor technique in DC link of three-phase PWM-VS inverters: a review and a novel solution. IEEE Trans. IA., 33 (5): 1241-1253.

[9] P. Pillay, R. Krishnan, 1989. Modeling, simulation, and analysis of permanent-magnet motor drives. II: The Brushless DC Motor Drive. IEEE Trans. Ind. Appl., 25 (2): 274-279.

[10] J. P. Jahnson, M. Ehsani, and Y. Guzelaunler, 1999. Review of sensorless methods for brushless DC. in Proc. IEEE IAS Annu. Meeting Conf., Phoenix, AZ, 143–150.

[11] Q. Jiang, C. Bi, and R. Huang, 2005. A new phase-delay method to detect back EMF zero-crossing points for sensorless control of spindle motors. IEEE Trans. Magnetics, 41 (7): 2287–2594.

[12] A. H. Niasar, A. Vahedi, and H. Moghbeli, 2008. A novel position sensorless control of a four-switch, brushless DC motor drive without phase shifter. IEEE Trans. Power Electron., 23 (6): 3079–3087.

[13] R. C. Becerra, T. M. Jahns, and M. Ehsani, 1991. Four-quadrant sensorless brushless ECM drive. in Proc. APEC'91, 202–209.

[14] J. Moreira, 1996. Indirect sensing for rotor flux position of permanent magnet AC motors operating over a wide speed range. IEEE Trans. Ind. Appl., 32 (6): 1394–1401.

[15]S. Ogasawara and H. Akagi, 1991. An approach to position sensorless drive for brushless dc motors. IEEE Trans. Ind. Appl., 27 (5): 928–923.

[16]J. Shao, D. Nolan, and T. Hopkins, 2002. A novel direct back EMF detection for sensorless brushless DC (BLDC) motor drives. in Proc. IEEE Appl. Power Electron. Conf. Expo., 1: 33–37.

[17]G. J. Su and W. McKeever, 2004. Low-cost sensorless control of brushless DC motors with improved speed range. IEEE Trans. Power Electron., 19 (2): 296–302.

[18]Miller I. Brushless permanent-magnet and reluctance motor drives. Oxford: Clarendon Press, Book Style; 1989.

[19]J. Kennedy, R. Eberhart, 1995. Particle Swarm Optimization. in Proc. IEEE International Conference on Neural Networks, 1942-1948.

[20]M. El-Sharkawi, K. Lee, 2008. Fundamentals of Particle Swarm Optimization Techniques. IEEE, 1nd edition, 71-87.

[21]Zee-Lee Gaing, 2004. A Particle Swarm Optimization Approach for Optimum Design of PID controller in AVR system. IEEE Trans. Energy Conversion, 19 (2): 384-391.

[22]P. Damodharan and K. Vasudevan, 2010. Sensorless Brushless DC Motor Drive Based on the Zero-Crossing Detection of Back Electromotive Force (EMF) From the Line Voltage Difference. IEEE Trans. Energy Conversion., 25 (3): 661–668.

[23]J.Johnson, 1999. Review of Sensorless Methods for Brushless DC. IAS, 143-150.

[24]Y.-S. Lai and Y.-K. Lin, 2006. Assessment of pulse-width modulation techniques for brushless DC motor drives. in Conf. Rec. IAS Annual Meeting 2006, 1629-1636.

[25]J.-H. Song and I. Choy, 2004. Commutation torque ripple reduction in brushless DC motor drives using a single current sensor. IEEE Trans. Power Electronics, 19 (2): 312-319.

[26]K.-H. Kim, M.-J. Youn, 2002. Performance comparison of PWM inverter and variable Dc link inverter schemes for high-speed sensorless control of BLDC motor. Electronics Letters, 38 (21): 1294-1295.

[27]Q. Li, H. Huang, B. Yin, 2008. The study of PWM methods in permanent magnet brushless DC motor speed control system. International Conference on Electrical Machines and Systems ICEMS 2008, 3897-3900.